Heterogeneous Catalysis Hot Paper

International Edition: DOI: 10.1002/anie.201806354
German Edition: DOI: 10.1002/ange.201806354

Capturing the Genesis of an Active Fischer–Tropsch Synthesis Catalyst with Operando X-ray Nanospectroscopy

*Ilse K. van Ravenhorst[+], Charlotte Vogt[+], Heiko Oosterbeek, Koen W. Bossers, José G. Moya-Cancino, Alexander P. van Bavel, Ad M. J. van der Eerden, David Vine, Frank M. F. de Groot, Florian Meirer, and Bert M. Weckhuysen**

Abstract: *A state-of-the-art operando spectroscopic technique is applied to Co/TiO_2 catalysts, which account for nearly half of the world's transportation fuels produced by Fischer–Tropsch catalysis. This allows determination of, at a spatial resolution of approximately 50 nm, the interdependence of formed hydrocarbon species in the inorganic catalyst. Observed trends show intra- and interparticular heterogeneities previously believed not to occur in particles under 200 μm. These heterogeneities are strongly dependent on changes in H_2/CO ratio, but also on changes thereby induced on the Co and Ti valence states. We have captured the genesis of an active FTS particle over its propagation to steady-state operation, in which micrograd ients lead to the gradual saturation of the Co/TiO_2 catalyst surface with long chain hydrocarbons (i.e., organic film formation).*

Heterogeneous catalytic reactions such as the Fischer–Tropsch synthesis (FTS) of long-chain hydrocarbons are dynamic and complex, often comprised of inorganic (catalyst) and organic parts (reactants and products). Conventional and widely applied spectroscopic techniques often focus on either the organic part (e.g., vibrational spectroscopy) or on the inorganic part (e.g., X-ray spectroscopic techniques). The combination of both inorganic and organic information shows great promise to answer long-standing questions about complex catalytic reactions. The FTS propagates through a complex surface polymerization process of adsorbed C_1 reaction intermediates derived from synthesis gas (a mixture of CO and H_2).[1–7] Cobalt-based FTS catalysts are an integral part of this gas-to-liquid (GTL) process because of their high wax selectivity and relatively high stability.[8,9] The activation and deactivation of these cobalt nanoparticles supported on an inorganic oxide, such as Al_2O_3 or TiO_2, is believed to occur through a multitude of mechanisms, however consensus in literature is often still lacking. While the literature is imbued with proposed deactivation mechanisms,[5,10,11] the equally interesting catalyst activation period is often overlooked.[12,13] During the day(s)-long activation or induction period (which is highly dependent on reaction conditions and the catalyst), FTS catalyst particles are believed to be gradually saturated by a film of long-chain hydrocarbons, followed by pore filling through which further reactants must diffuse.[12,14,15] The complexity of the FTS process is also captured in the myriad of proposed deactivation mechanisms, which are generally related to the conversion of the active phase, considered as metallic cobalt, into an inert phase. For example, cobalt reoxidation or carburization,[16,17] the formation of support oxide–cobalt species occurring through strong metal–support interactions (SMSI),[8,18,19] the loss of active cobalt surface area arising from crystalline growth (i.e., metal sintering),[11,20–22] and finally fouling for example by hydrocarbon deposition in the form of various carbon species formed at the cobalt surface.[11,23–25]

The dynamic interplay of these different activation and deactivation mechanisms necessitates studies under—or approaching—true reaction conditions. Passivation, or for example, changes in the sample's gaseous environment can significantly alter the state of a FTS catalyst, and hence have to date prevented a complete understanding of the catalyst material under relevant conditions.[26–29] Operando characterization studies can greatly advance our knowledge of working catalyst systems providing nanoscale chemical information on both the organic (products and reaction intermediates) and the inorganic (metal and support) constituents of the catalyst material under operating conditions (i.e., high temperatures and pressures and reactants).[30] The development of scanning transmission X-ray microscopy (STXM), which is a combination of microscopy and X-ray absorption spectroscopy, under operating conditions and with on-line activity data, presents the imperative qualities necessary for understanding complex catalytic systems.

In this work, we present an operando STXM study of a Co/TiO_2 FTS catalyst operated under various FTS conditions (493 K, 1–4 bar and 1:1, and 2:1 H_2/CO feed) over extended periods of time (i.e., 3 days). The technique allows mapping of single catalyst particles (i.e., several Co nanoparticles supported on grains of TiO_2, schematic in Figure 1 and STEM-EDX in Figure S2) at a spatial resolution of approximately 50 nm in the soft X-ray regime (200–2000 eV), which offers the unique ability to detect both the full range of

[*] I. K. van Ravenhorst,[+] C. Vogt,[+] K. W. Bossers, J. G. Moya-Cancino, A. M. J. van der Eerden, Prof. Dr. F. M. F. de Groot, Dr. F. Meirer, Prof. Dr. Ir. B. M. Weckhuysen
Inorganic Chemistry and Catalysis group
Debye Institute for Nanomaterials Science, Utrecht University
Universiteitsweg 99, 3584 CG Utrecht (The Netherlands)
E-mail: B.M.Weckhuysen@uu.nl

H. Oosterbeek, Dr. Ir. A. P. van Bavel
Shell Global Solutions International B.V.
Grasweg 31, 1031 HW Amsterdam (The Netherlands)

Dr. D. Vine
ALS beamline 11.0.2, Lawrence Berkeley National Laboratory
1 Cyclotron Road, Berkeley, 94720 CA (USA)

[+] These authors contributed equally to this work.

Supporting information and the ORCID identification number(s) for the author(s) of this article can be found under: https://doi.org/10.1002/anie.201806354.

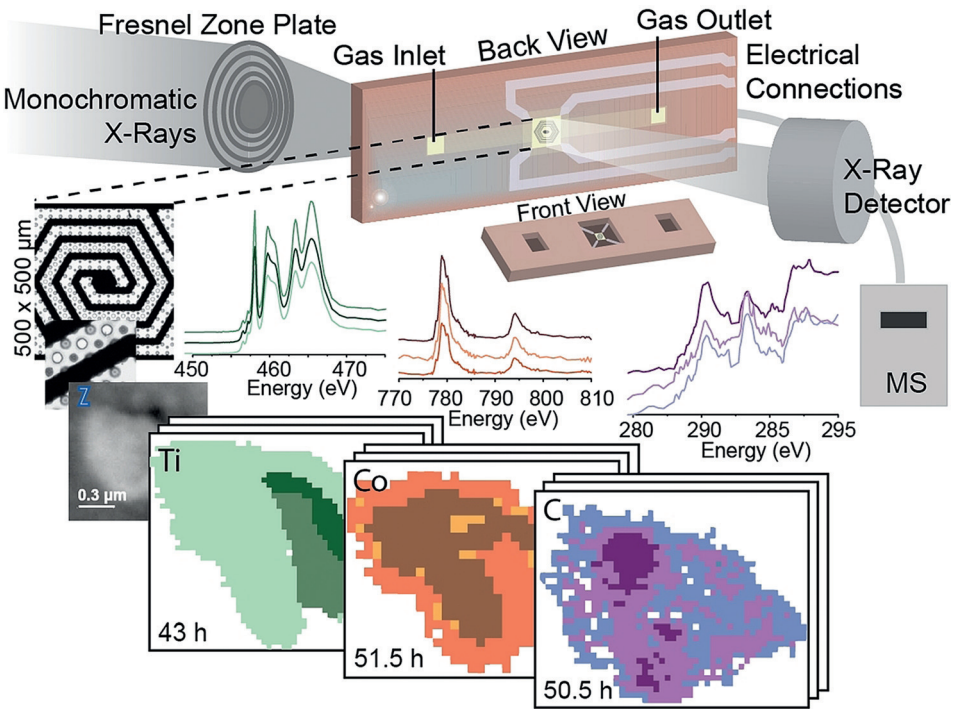

Figure 1. Overview of the operando MEMS reactor and related data acquisition method by STXM for measuring a 15 wt% Co/TiO_2 catalyst material. Top: schematic representation of the MEMS reactor used in this work. Bottom-left: optical microscopy photograph of heating spiral with 0.1 µm overall thickness, with SiN_x windows of 15 nm thickness containing the single Co/TiO_2 catalyst particles. Bottom: data acquisition method, the focused soft X-ray beam is changed in energy by the monochromator to measure an X-ray absorption spectrum for each pixel as a function of time-on-stream. The Co nanoparticles are well distributed over the TiO_2 support as can be seen from the Ti and Co maps.

reactants and intermediates (through the C K-edge), and the inorganic constituents of the catalyst (through both the Co and Ti $L_{2,3}$-edges) including their chemical state. Along with on-line product analysis by mass spectrometry (MS), this approach is highly suitable for an in-depth operando nano-spectroscopy study. The main challenge that arises with the use of STXM is the strong absorption of the relatively low-energy synchrotron photons needed to study for example, the C K-edge, limiting the thickness of samples that can be analyzed. For this reason we used a micro-electromechanical systems (MEMS) reactor, which allows measurement of individual catalyst particles at both elevated temperatures and pressures[26,31] (Figure 1).

The Co/TiO_2 FTS catalyst was characterized and tested by XRD, H_2-TPR, SEM-EDX, and N_2-sorption, and details of these characterization data can be found in the Supporting information. Furthermore, the catalysts were extensively tested in a classical fixed-bed reactor setup (high-throughput setup by Avantium). Figure 2 shows the activity data for the 15 wt% Co/TiO_2 catalyst samples tested at 1:1 H_2/CO ratio. Every hour, the reaction products were analyzed by on-line gas chromatography (Varian 430 GC; Figure 2a–d summarizes the activity, selectivity, paraffin to olefin ratios, chain-growth probability and Co time-yield (CTY, moles $CO\,g_{Co}^{-1}\,s^{-1}$)) versus time. Industrial FTS catalysts often run for weeks or months on end, yet in the first few days of catalytic testing we can already see a drop in activity and a change in selectivity (Figure 2). Though technically a loss in activity such as that observed can be described as deactivation; this initial loss in activity can also be seen as activation; "breaking-in" of the catalyst particle,[14,15] or the propagation of the catalyst system to steady state operation as evidenced by a decline of the slope in activity in Figure 2a (up to 90 hours), and Figure S20 for 275 h. The selectivity to methane (C_1), C_2–C_4, and C_{5+} FTS products stabilize in the steady-state at 10%, 15% and 75%, respectively (Figure 2b). Deactivation rather, is the irreversible formation of for example, carbides, graphite, or for example white coke,[1] which further decreases the catalytic activity from steady-state operation to lower, or no activity.

As this activation period is often overlooked or incorrectly assumed to be deactivation, it can provide clues to the overall working state of the industrial FTS catalyst. We thus set out to investigate this up to 50–60 hour period with operando STXM; over the onset of steady-state catalysis during the first few days of FTS operation.

In the Supporting Information (see section "Supplemental results of particles X and Y"), a set of tests are presented that determine the setup's responsivity and to verify whether the conditions we apply are those of a working catalyst by performing operando STXM measurements with several

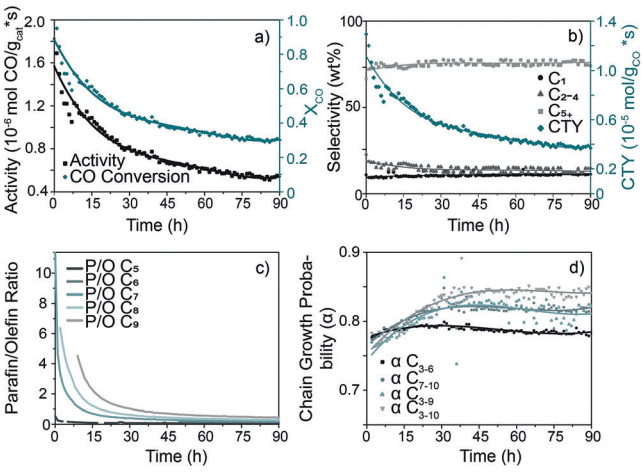

Figure 2. Activity and selectivity for the 15 wt% Co/TiO_2 catalyst tested in a classical plug-flow reactor setup for 90 h of FTS under 1:1 ratio of H_2/CO.

catalyst particles. Feedstock switches between 2:1 and 1:1 H_2/CO are shown to correspond to spectral features, and mass spectrometry data. Furthermore, an indication of a correlation between a slightly higher Co valence state and C buildup was found.

After confirming that the FTS operando STXM system worked, we further performed in situ measurements on a new catalytic reactor in order to examine the gradual activation of the FTS catalyst. Before catalysis, the state of Co in the catalyst was characterized by STXM at room temperature under He flow (fresh and reduced particles in Figure 3). During catalysis, the C K-edge, Co $L_{2,3}$-edges (Figures S13–16, S22–24) and Ti $L_{2,3}$-edges (Figure S26 and S27) were recorded consecutively. The catalyst was reduced at 723 K for 16 h under 1 bar of H_2.

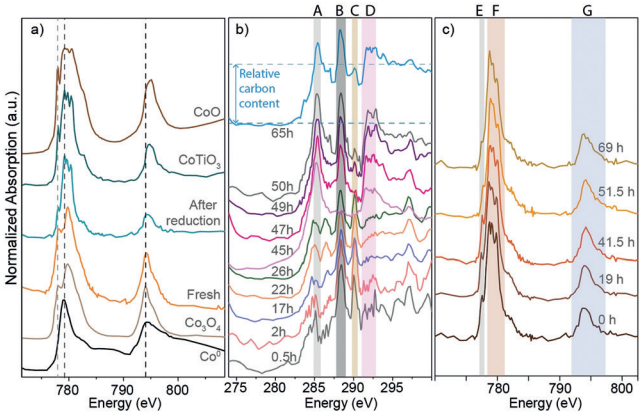

Figure 3. a) In situ bulk C K-edge spectra of 15 wt% Co/TiO_2 FTS particle X followed with STXM as a function of increasing time-on-stream in MEMS reactor 1. b) Same as (a) for catalyst particle Z in MEMS reactor 2. Shown in blue is the method used to determine the relative carbon content in non-normalized spectra (shown here are normalized spectra). c) In situ bulk Co $L_{2,3}$-edge spectra of catalyst particle Z as a function of increasing time-on-stream. The relative carbon content is based on the intensity of the edge-jump as indicated above in (b). The colored bars indicate the different characteristic regions, A: olefinic carbon or π-transitions, B: aliphatic carbon or σ*-transitions, C: O π* of oxygenated carbon, and D: general hydrocarbon for the carbon K-edge. E: pre-edge region, F: tri-peak edge, and G: L_2-edge for the Co L-edges.

The catalyst particle hereby produced will be referred to as Z, shown in Figure 1–4 and elaborated on in the Supporting Information "Supplemental results of particle Z". Temperatures and pressures were chosen to mimic those employed for the classical fixed-bed study, although it must be noted that the gas hourly space velocities will inherently be different because of the small volume of the nanoreactor employed in the STXM study.

Based on the measured Co $L_{2,3}$-edge spectra of catalyst particle Z in Figure 3a, it can be concluded that the catalyst particle is reduced with respect to the initial state. However, it also contains some features which relate to slightly higher Co valence states as can be seen in the reference spectra (Figure 3a) but is not unusual based on previous work on Co/TiO_2 FTS catalysis.[27,29,32–34] We believe uncertainties in normalization of the soft-XAS (e.g., unknown contributions of metallic and Co^{2+} and the required knowledge thereof to properly normalize) are prone to misrepresentation of the observed spectral features making a true quantitative analysis of the oxidation states impossible. However, qualitative features such as for example, the narrow L_3-edge with a tripeak edge feature allow us to discern the presence of a high degree of metallic Co in catalyst particle Z, but with a higher amount of Co^{2+} species than particles X and Y. The reduction behavior of Co/TiO_2 catalysts follow a two-step process. The first step consists of the reduction of Co_3O_4 into CoO, followed by the reduction from CoO to metallic Co. This second step only starts when all the Co_3O_4 is converted. Thus no Co^{3+} is present in the catalyst.

The cobalt and carbon XANES for particle Z are displayed in Figure 3. These spectra were averaged over the whole catalyst particles, and thus contain no spatial information. However, from Figure 3, it already becomes clear that the overall amount of C species (edge-jump) is increasing which is an indication of the gradual saturation of the catalyst particle pores with hydrocarbons (hydrocarbon film).[14,15]

Table S1 lists important observed features and their spectral assignment as used in this work. For example, conjugated or unsaturated carbonaceous species (with a characteristic X-ray absorption feature at 285 eV), increase with increasing reaction time. It is important to note here that the gradual build-up of hydrocarbon deposits correlates well to the time period for what has been defined as the activation, or "breaking-in" period, where the gradual saturation of the different catalyst particles with hydrocarbon deposits occurs (Figure 2, and Figure 3).[14] Furthermore, we observe an overall increase of a multitude of hydrocarbon species with C–C bonds (characteristic spectral features in the range of 291–293.5 eV). From the ratio between the C=C π* features at 285 eV and the C–H σ* features around 288 eV, we know that with increasing time-on-stream these hydrocarbon deposits vary greatly in degree of saturation (Figure 3). In the following we discuss the effect of localized heterogeneities in the degree of reduction/oxidation in Co/TiO_2 FTS catalysts by examining the C K-edge spectra in more detail. Figure 4 shows the sequence of the chemical maps generated from PCA and subsequent clustering evaluated at the C K-edge recorded for the particle under working conditions, adding spatial information to the C K-edge spectra displayed in Figure 3b. The first carbonaceous species, detected after 0.5 h, are O-containing ones, as evidenced by the distinct feature at 290 eV. Precursors to olefinic species seemed to be more in the shell of the catalyst particle (that is, the outer part of the porous, 1 μm large Co/TiO_2 particle) after 17 h time-on-stream. Particles of this size are not expected to be limited by (reactant) diffusion,[35,36] however slight heterogeneities in the distribution of Co nanoparticles on the TiO_2 support are likely to cause localized long-chain hydrocarbon deposit build-up. The relatively low pressure of these experiments is in agreement with this explanation, as higher pressure would facilitate their solubility in the film. Furthermore, the C K-edge peaks at 288 and 290 eV become increasingly pronounced, indicating the presence of more aliphatic CH_x species. The presence of more unsaturated, either aromatic

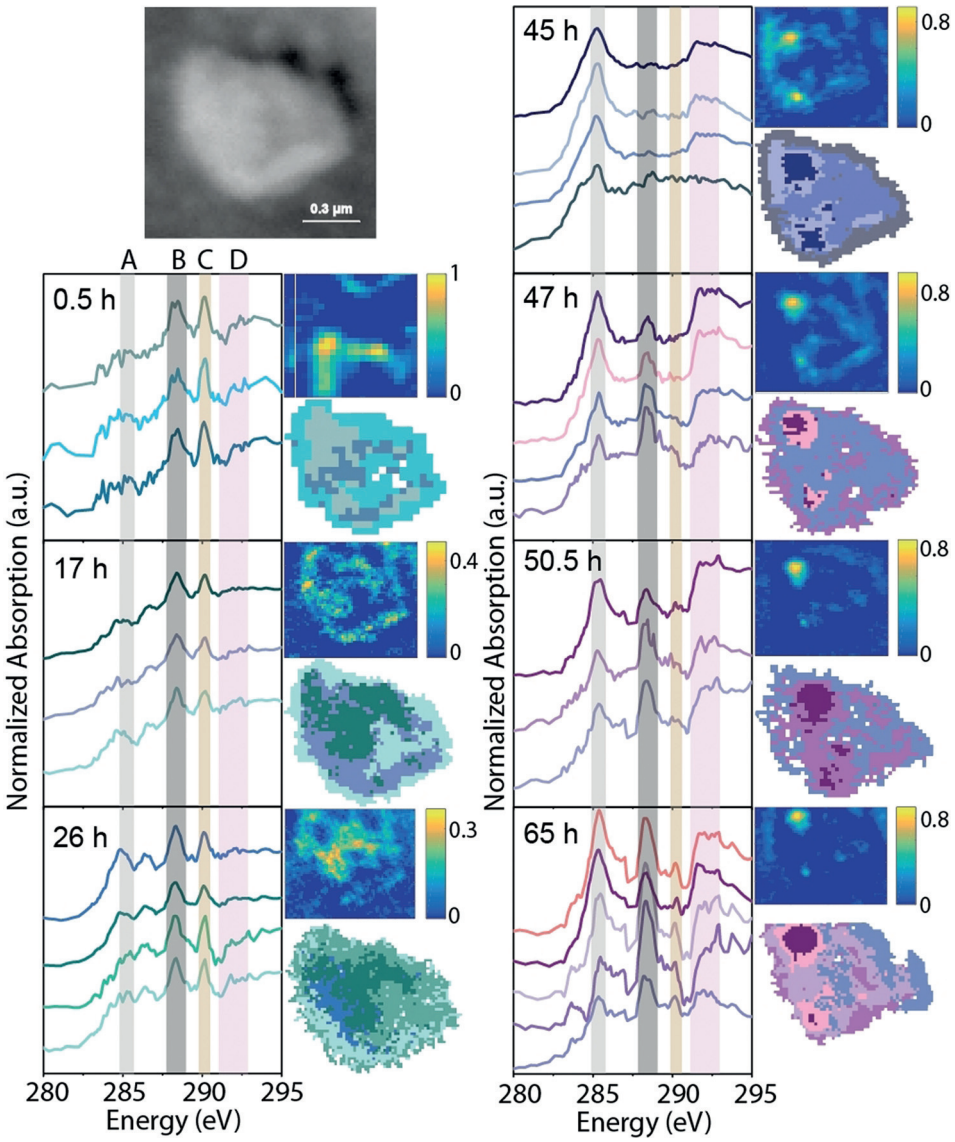

Figure 4. Sequence of chemical maps of particle Z, based on C K-edge spectra obtained via PCA and clustering, and corresponding C intensity maps (based on the intensity of the edge-jump in each pixel of the map), of a single Co/TiO_2 FTS particle evolving over 3 days as imaged by in situ STXM at a reaction temperature of 493 K, atmospheric pressure and a H_2/CO ratio of 1:1. A: olefinic carbon or π-transitions, B: aliphatic carbon or σ*-transitions, C: O π* of oxygenated carbon, and D: general hydrocarbon.

or olefinic in nature, carbon-containing species are more marked in the core of the Co/TiO_2 catalyst particle, whereas in the shell of the catalyst particle, saturated C–C σ-transitions arise. The presence of a second feature at 286.5 eV, which is already visible at 17 h, becomes more pronounced after 26 h time-on-stream, and indicates the presence of polynuclear aromatic, or highly unsaturated hydrocarbon species.

After 26 h time-on-stream, the shell-like structure of the hydrocarbon species' distribution becomes even more visible. As also previously noted by our group, operando Raman spectroscopy can show that the nature of hydrocarbon deposits clearly changes over the first days of FTS.[32] Additionally, a larger edge-jump towards the inner core of the catalyst particle indicates the formation of more C-containing species at this location as can be seen in the carbon intensity maps in Figure 4. These maps were based on the edge-jump magnitude of each pixel, for each chemical image sequence. Interestingly, after 45 h of FTS, an intermediate state of hydrocarbon species is observed, where all-aliphatic C–H species are consumed in the production of unsaturated and saturated C–C carbonaceous species. Furthermore, this "transition phase", where most carbonaceous species are unsaturated, is shown to be primarily located within the inner core of the catalyst particle. Interestingly, thus it appears that reduction of the higher Co valence state (suboxide species), based on Co spectra in Figure 3c is correlated to the hydrocarbon transition phase. That is, the particle contains more Co^0 (that is, metallic or carbidic Co, as no distinction can be made from Co $L_{2,3}$ spectra alone) between 40–50 h, and subsequent saturation of hydrocarbon species on the particle may bolster findings in that literature that suggest suboxide species are promotors for olefinic hydrocarbon synthesis in FTS.[32] However, it is also plausible that the gradual saturation of the hydrocarbon "film" on the catalyst surface emerges from the inside outwards leaves more time for the reinsertion and hydrogenation of unsaturated hydrocarbons on the outside of the particle.[14,15]

The relative amount of hydrogen in the hydrocarbon species after 45 h is low, as the corresponding aliphatic C–H, and COOH features between 287–289 eV are absent. The ratio of olefinic to aliphatic species is plotted in Figure S24. Here, this transition phase can also clearly be seen to emerge at around 45 h time-on-stream. It should be noted that in STXM analysis, I_0, which is used to determine the OD of the sample, is obtained from the area without sample in the same field of view. Contributions to absorption that are not caused by the sample (e.g., from reactor windows, surrounding gases, etc.) are therefore removed. Thus we expect no contribution of for example, gaseous CO to the C spectra.

Furthermore, at 45 h of FTS it is clear that unsaturated hydrocarbon species occur more towards the outside of the Co/TiO_2 catalyst particle, while the particle core contains unsaturated as well as C–C single bonds.

Finally, at a reaction time of 45 h and beyond, there is an indication of O-containing aromatic species, such as benzoquinone-type species,[37–40] in the shell of the catalyst particle, which are commonly linked to an X-ray absorption edge-shoulder feature at 284.2 eV, although the true origin of this species cannot yet be provided. This trend is further noticed in all subsequent spectral image sequences up to 65 h. Furthermore, at and after 45 h of reaction we observe two clear core–shell-like features, which are consequently clustered in the same or similar location on the catalyst particle (i.e., the two dark circular areas on the clustered chemical maps). Furthermore, the fact that this intensity is present both in clustered data, and in the carbon K-edge-jump intensity maps plotted in Figure 4, tells us that these species are not only chemically different, but there is also more carbon present where these species are located. Interestingly these spots are also seen in the Co chemical images from the start of the FTS reaction, and they correlate to a higher edge-jump, or more cobalt (Figure S24). The fact that these spots merge after 51.5 h can indicate the redistribution of cobalt, which is linked to the formation of carbon in Figure 4, consistent with previous findings from our group.[27]

Additionally, in Figure 4 a small feature at 288.3 eV emerges inwards, from the particle shell to the particle core, which is continued at 47 h in Figure 4. Thus it seems that hydrogenation of the unsaturated carbon-containing species occurs from the outside inwards, that is, from the particle surface to the particle core. One may argue that the two spots, which continue to appear after 45 h of FTS onwards may be due to a thickness effect or an attenuation length issue as these features both appear near the core of the particle. However, no pre-edge oversaturation was observed and optical density was corrected for (see section "Data Analysis" in the Supporting Information).

In summary, from this operando nanospectroscopic study of chemically speciated carbonaceous deposits of a working Co/TiO_2 Fischer–Tropsch catalyst, we can conclude that hydrocarbon deposits (differing in their chemical composition) form a film on the surface of the catalyst particle, with inter- and intraparticle heterogeneities. These heterogeneities can be correlated to slight changes in the local Co oxidation/valence states. Furthermore, the gradual build-up and shift from short-chain hydrocarbons to longer-chain hydrocarbons is shown to occur. Furthermore, as evidenced by particles X and Y (discussed in the Supplementary information), compared to particle Z (discussed in the main text), the catalyst particle with slightly higher Co valence state, hydrocarbon build-up becomes significant. This suggests slight oxidation is closely related to catalyst α, as previously suggested.[14,15] In fact, the presence of higher Co valence state can be correlated to the degree of saturation in the observed carbon species. Further investigation is necessary to determine whether this relationship is causal or merely correlative. Our data further suggest that much of the ongoing debate in literature with respect to location and type of coke species can be sparked by slight changes in the local oxidation state of cobalt, even within one catalyst particle and sample.

Acknowledgements

B.M.W. thanks the Netherlands Organization for Scientific Research (NWO) and Shell Global Solutions International B.V. for a CHIPP research grant as well as NWO for a Gravitation program (Netherlands Center for Multiscale Catalytic Energy Conversion (MCEC)). Dr. B. Morana and Dr. G. Pandraud (Else Kooi Lab, TUDelft, The Netherlands) are acknowledged for providing the nanoreactors and useful insights. Dr. S. R. Bare (SLAC, USA) is thanked for carefully reading the manuscript before submission. Prof. A. P. Hitchcock (McMaster University, Canada) is thanked for help with the assignment of XAS features.

Conflict of interest

The authors declare no conflict of interest.

Keywords: chemical imaging · Fischer–Tropsch synthesis · heterogeneous catalysis · nanoparticles · X-ray microspectroscopy

How to cite: *Angew. Chem. Int. Ed.* **2018**, *57*, 11957–11962
Angew. Chem. **2018**, *130*, 12133–12138

[1] G. Ertl, H. Knözinger, F. Schüth, J. Weitkamp, *Handbook of Heterogeneous Catalysis*, Wiley-VCH, Weinheim, **1997**.
[2] Z.-P. Liu, P. Hu, *J. Am. Chem. Soc.* **2002**, *124*, 11568–11569.
[3] S. J. Jenkins, D. A. King, *J. Am. Chem. Soc.* **2000**, *122*, 10610–10614.
[4] S. E. Colley, R. G. Copperthwaite, G. J. Hutchings, S. P. Terblanche, M. M. Thackeray, *Nature* **1989**, *339*, 129–130.
[5] N. E. Tsakoumis, M. Rønning, Ø. Borg, E. Rytter, A. Holmen, *Catal. Today* **2010**, *154*, 162–182.
[6] A. Y. Khodakov, W. Chu, P. Fongarland, *Chem. Rev.* **2007**, *107*, 1692–1744.
[7] G. L. Bezemer, J. H. Bitter, H. P. C. E. Kuipers, H. Oosterbeek, J. E. Holewijn, X. Xu, F. Kapteijn, A. J. van Dillen, K. P. de Jong, *J. Am. Chem. Soc.* **2006**, *128*, 3956–3964.
[8] D. Schanke, A. M. Hilmen, E. Bergene, K. Kinnari, E. Rytter, E. Adnanes, A. Holmen, *Energy Fuels* **1996**, *10*, 867–872.
[9] W. Ma, G. Jacobs, D. E. Sparks, M. K. Gnanamani, V. R. R. Pendyala, C. H. Yen, J. L. S. Klettlinger, T. M. Tomsik, B. H. Davis, *Fuel* **2011**, *90*, 756–765.
[10] P. J. Van Berge, J. Van De Loosdrecht, S. Barradas, A. M. Van Der Kraan, *Catal. Today* **2000**, *58*, 321–334.
[11] A. M. Saib, D. J. Moodley, I. M. Ciobîc, M. M. Hauman, B. H. Sigwebela, C. J. Weststrate, J. W. Niemantsverdriet, J. Van De Loosdrecht, *Catal. Today* **2010**, *154*, 271–282.
[12] D. Vervloet, F. Kapteijn, J. Nijenhuis, J. R. van Ommen, *Catal. Sci. Technol.* **2012**, *2*, 1221–1233.
[13] M. Luo, R. J. O'Brien, S. Bao, B. H. Davis, *Appl. Catal. A* **2003**, *239*, 111–120.
[14] E. W. Kuipers, C. Scheper, J. H. Wilson, I. H. Vinkenburg, H. Oosterbeek, *J. Catal.* **1996**, *158*, 288–300.
[15] E. W. Kuipers, I. H. Vinkenburg, H. Oosterbeek, *J. Catal.* **1995**, *152*, 137–146.
[16] G. Jacobs, P. M. Patterson, Y. Zhang, T. Das, J. Li, B. H. Davis, *Appl. Catal. A* **2002**, *233*, 215–226.
[17] A. Tavasoli, R. M. Malek Abbaslou, A. K. Dalai, *Appl. Catal. A* **2008**, *346*, 58–64.
[18] G. Kiss, C. E. Kliewer, G. J. DeMartin, C. C. Culross, J. E. Baumgartner, *J. Catal.* **2003**, *217*, 127–140.

[19] W. Zhou, J. G. Chen, K. G. Fang, Y. H. Sun, *Fuel Process. Technol.* **2006**, *87*, 609 – 616.
[20] C. J. Bertole, C. A. Mims, G. Kiss, *J. Catal.* **2002**, *210*, 84 – 96.
[21] M. Claeys, M. E. Dry, E. Van Steen, P. J. Van Berge, S. Booyens, R. Crous, P. Van Helden, J. Labuschagne, D. J. Moodley, A. M. Saib, *ACS Catal.* **2015**, *5*, 841 – 852.
[22] E. Van Steen, M. Claeys, M. E. Dry, J. Van De Loosdrecht, E. L. Viljoen, J. L. Visagie, *J. Phys. Chem. B* **2005**, *109*, 3575 – 3577.
[23] D. J. Moodley, J. van de Loosdrecht, A. M. Saib, M. J. Overett, A. K. Datye, J. W. Niemantsverdriet, *Appl. Catal. A* **2009**, *354*, 102 – 110.
[24] D. K. Lee, J. H. Lee, S. K. Ihm, *Appl. Catal.* **1988**, *36*, 199 – 207.
[25] W. Chen, I. A. W. Filot, R. Pestman, E. J. M. Hensen, *ACS Catal.* **2017**, *7*, 8061 – 8071.
[26] E. de Smit, I. Swart, J. F. Creemer, G. H. Hoveling, M. K. Gilles, T. Tyliszczak, P. J. Kooyman, H. W. Zandbergen, C. Morin, B. M. Weckhuysen, F. M. F. de Groot, *Nature* **2008**, *456*, 222 – 225.
[27] K. H. Cats, J. C. Andrews, O. Stéphan, K. March, C. Karunakaran, F. Meirer, F. M. F. de Groot, B. M. Weckhuysen, *Catal. Sci. Technol.* **2016**, *6*, 4438 – 4449.
[28] I. D. Gonzalez-Jimenez, K. Cats, T. Davidian, M. Ruitenbeek, F. Meirer, Y. Liu, J. Nelson, J. C. Andrews, P. Pianetta, F. M. F. De Groot, B. M. Weckhuysen, *Angew. Chem. Int. Ed.* **2012**, *51*, 11986 – 11990; *Angew. Chem.* **2012**, *124*, 12152 – 12156.
[29] K. H. Cats, I. D. Gonzalez-Jimenez, Y. Liu, J. Nelson, D. van Campen, F. Meirer, A. M. J. van der Eerden, F. M. F. de Groot, J. C. Andrews, B. M. Weckhuysen, *Chem. Commun.* **2013**, *49*, 4622 – 4624.
[30] E. de Smit, B. M. Weckhuysen, *Chem. Soc. Rev.* **2008**, *37*, 2758 – 2781.
[31] J. F. Creemer, F. Santagata, B. Morana, L. Mele, T. Alan, E. Iervolino, G. Pandraud, in *MEMS 2011, Cancun, Mex. January 23 – 27* **2011**, pp. 1103 – 1106.
[32] K. H. Cats, B. M. Weckhuysen, *ChemCatChem* **2016**, *8*, 1531 – 1542.
[33] F. Morales, E. de Smit, F. M. F. de Groot, T. Visser, B. M. Weckhuysen, *J. Catal.* **2007**, *246*, 91 – 99.
[34] F. Morales, F. M. F. De Groot, O. L. J. Gijzeman, A. Mens, O. Stephan, B. M. Weckhuysen, *J. Catal.* **2005**, *230*, 301 – 308.
[35] E. Iglesia, S. L. Soled, J. E. Baumgartner, S. C. Reyes, *J. Catal.* **1995**, *153*, 108 – 122.
[36] R. B. Anderson, B. Seligman, J. F. Shultz, R. Kelly, M. A. Elliott, *Ind. Eng. Chem. Res.* **1952**, *44*, 391 – 397.
[37] P. R. Haberstroh, J. A. Brandes, Y. Gélinas, A. F. Dickens, S. Wirick, G. Cody, *Geochim. Cosmochim. Acta* **2006**, *70*, 1483 – 1494.
[38] G. D. Cody, H. Ade, S. Wirick, G. D. Mitchell, A. Davis, *Org. Geochem.* **1998**, *28*, 441 – 455.
[39] J. T. Francis, A. P. Hitchcock, *J. Phys. Chem.* **1992**, *96*, 6598 – 6610.
[40] N. A. Hughes, V. Gloriot, D. D. Smiley, G. Jacobs, V. R. R. Pendyala, W. Graham, U. M. Ma, M. K. Gnanamani, W. D. Shafer, A. Maclennan, Y. Hu, et al., in *Fischer-Tropsch Synthesis, Catalysts, and Catalysis: Advances and Applications* (Ed.: B. H. Davis, M. L. Occelli), CRC Press, Taylor & Francis Group, Boca Raton, FL, USA, **2016**, pp. 85 – 106.

Manuscript received: June 4, 2018
Accepted manuscript online: August 2, 2018
Version of record online: August 17, 2018

